論文 / 著書情報
Article / Book Information

Title	Design of Non-Separable 3-D QMF Banks Using McClellan Transformations
Authors	Toshiyuki YOSHIDA, Todor Cooklev, AKINORI NISHIHARA, NOBUO FUJII
Citation	IEICE Trans. Fundamentals, Vol. E79-A, No. 5, pp. 716-720
Pub. date	1996, 5
URL	http://search.ieice.org/
Copyright	(c) 1996 Institute of Electronics, Information and Communication Engineers

LETTER

Design of Non-Separable 3-D QMF Banks Using McClellan Transformations

Toshiyuki YOSHIDA[†], Todor COOKLEV[†], Akinori NISHIHARA[†], *and* Nobuo FUJII[†], *Members*

SUMMARY This paper proposes a design technique for 3-D non-separable QMF banks with Face-Centered Cubic Sampling (FCCS) and Body-Centered Cubic Sampling (BCCS). In the proposed technique, 2-D McClellan transformation is applied to a suitably designed 2-D prototype QMF to obtain 3-D QMFs. The design examples given in this paper demonstrate advantages of the proposed method.
key words: *digital signal processing, multidimensional signal processing, QMF banks, McClellan transformation*

1. Introduction

Multidimensional Quadrature Mirror Filter (QMF) banks have many applications and continue to be studied extensively [1]–[3].

As in the 2-D case, 3-D QMFs are classified into separable and non-separable types. Since the design of separable QMFs, which can be realized by multiplying 1-D QMFs, is simple, they are used in many applications. In comparison with the separable case, although the design and implementation of non-separable QMFs is difficult, they offer more degrees of freedom [4], [5], which enables the shape of the decomposed subbands to closely match the human visual characteristics [6], [7]. This paper deals with a design of 3-D non-separable QMF banks. The 3-D QMFs designed in this paper are FCCS and BCCS-type QMFs, whose sampling schemes after downsampling correspond to FCCS and BCCS, respectively [6]–[9].

Sections 2 and 3 show the proposed design method for FCCS and BCCS-type QMFs, respectively, and design examples are given in Sect. 4. Finally, Sect. 5 concludes this paper.

2. Design of FCCS-Type QMF Banks

2.1 FCCS-Type Downsampling and QMF Banks

The FCCS-type downsampling process is shown in Fig. 1, where, for example,

$$\boldsymbol{D}_{FCCS} = \begin{bmatrix} 1 & 1 & 0 \\ 1 & 0 & 1 \\ 0 & 1 & 1 \end{bmatrix} \tag{1}$$

can be employed as the downsampling matrix $\boldsymbol{D}_{FCCS}$. Figure 2 illustrates several examples of baseband shapes for FCCS, where ω_{1c} indicates the intersection of each plane on the axis ω_1 [10].

Since $L = |\det \boldsymbol{D}_{FCCS}| = 2$, maximally-decimated QMF banks based on FCCS-type downsampling lead to two-channel QMF banks as shown in Fig. 3, where

$$\boldsymbol{\omega} = (\omega_1, \omega_2, \omega_2)^t, \qquad \boldsymbol{n} = (n_1, n_2, n_3)^t, \tag{2}$$

and $\boldsymbol{D}$ and $\boldsymbol{E}$ ($\equiv \boldsymbol{D}_{FCCS}$) are, respectively, the downsampling and upsampling matrices.

The total transfer function $Y(\boldsymbol{\omega})/X(\boldsymbol{\omega})$ can be easily found by making an extension of the 2-D case to 3-D, from which the perfect reconstruction condition can be obtained as

$$F_1(\boldsymbol{\omega})H_1(\boldsymbol{\omega}-\boldsymbol{\pi}) + F_2(\boldsymbol{\omega})H_2(\boldsymbol{\omega}-\boldsymbol{\pi}) = 0 \tag{3}$$

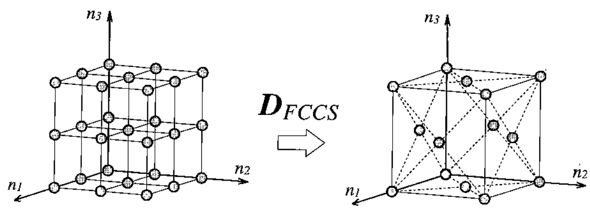

(a) (b)

Fig. 1 FCCS-type downsampling.

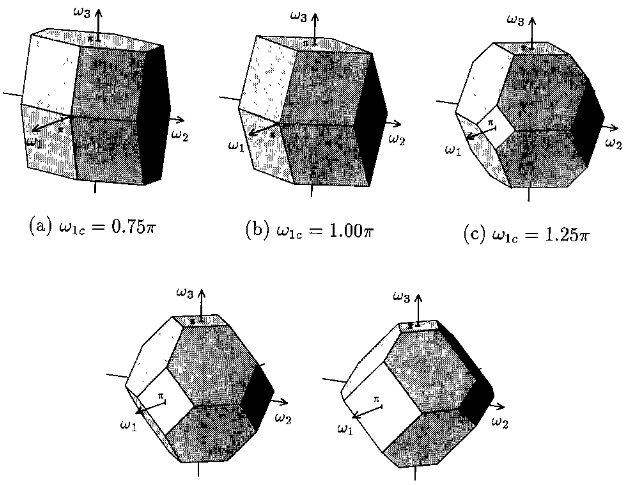

(a) $\omega_{1c} = 0.75\pi$ (b) $\omega_{1c} = 1.00\pi$ (c) $\omega_{1c} = 1.25\pi$

(d) $\omega_{1c} = 1.50\pi$ (e) $\omega_{1c} = 2.00\pi$

Fig. 2 Several possible baseband shapes for FCCS.

Manuscript received April 19, 1995.
Manuscript revised August 18, 1995.
[†]The authors are with the Faculty of Engineering, Tokyo Institute of Technology, Tokyo, 152 Japan.

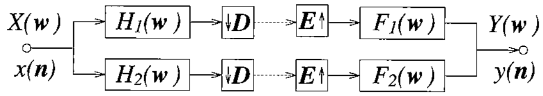

Fig. 3 Two-channel QMF bank.

$$F_1(\boldsymbol{\omega})H_1(\boldsymbol{\omega}) + F_2(\boldsymbol{\omega})H_2(\boldsymbol{\omega}) = \exp(-j\boldsymbol{p}^t\boldsymbol{\omega}), \quad (4)$$

where $\boldsymbol{\pi} = (\pi, \pi, \pi)^t$, and $\boldsymbol{p}$ is a constant vector corresponding to the system delay. Note that the gain constant $1/|\det \boldsymbol{D}|$ has been ignored for simplicity.

Although several design techniques have been proposed for 1-D and 2-D two-channel QMF banks [11], [12], a simple application of these techniques to 3-D case requires quite large amount of computations or results in rather unsatisfying frequency response with less degrees of freedom.

In the next section, a design technique will be proposed which overcomes these problems.

2.2 Proposed Design Method

In Refs. [8] and [10], the authors have proposed a design method for FCCS-type band-limiting filters, which is based on the 2-D McClellan transformation

$$\begin{aligned}\cos\omega &= F(\omega_2, \omega_2) \\ &= k\cos\omega_2 + (1-k)\cos\omega_2 \quad (0 < k < 1)\end{aligned} \quad (5)$$

on a suitably designed 2-D prototype filter $H(\omega_1, \omega)$. The proposed design technique is based on this idea.

This method requires a 2-D two-channel QMF bank as a prototype QMF bank. Now consider Fig. 3 as a 2-D two-channel QMF bank, where

$$\begin{cases} H_i(\boldsymbol{\omega}) = H_i(\omega_1, \omega) & (i = 1, 2) \\ F_i(\boldsymbol{\omega}) = F_i(\omega_1, \omega) & (i = 1, 2). \end{cases} \quad (6)$$

An FCCS-type QMF bank can be derived from the prototype 2-D QMF bank by applying the 2-D McClellan transformation $\cos\omega = F(\omega_2, \omega_2)$ as

$$\begin{aligned} &H_i(\omega_1, \omega_2, \omega_2) \\ &\quad = H_i(\omega_1, \omega)|_{\cos\omega = F(\omega_2, \omega_2)} \quad (i = 1,\ 2), \end{aligned} \quad (7)$$

$$\begin{aligned} &F_i(\omega_1, \omega_2, \omega_2) \\ &\quad = F_i(\omega_1, \omega)|_{\cos\omega = F(\omega_2, \omega_2)} \quad (i = 1,\ 2). \end{aligned} \quad (8)$$

We can easily verify this method because (3) leads to

$$\begin{aligned} &F_1(\omega_1, \omega_2, \omega_2)H_1(\omega_1 - \pi, \omega_2 - \pi, \omega_2 - \pi) \\ &\quad + F_2(\omega_1, \omega_2, \omega_2)H_2(\omega_1 - \pi, \omega_2 - \pi, \omega_2 - \pi) \\ &= \Big\{F_1(\omega_1, \omega)H_1(\omega_1 - \pi, \omega - \pi) \\ &\quad + F_2(\omega_1, \omega)H_2(\omega_1 - \pi, \omega - \pi)\Big\}\Big|_{\cos\omega = F(\omega_2, \omega_2)} \\ &= 0. \end{aligned} \quad (9)$$

In a similar way, (4) can be also proved, provided that the prototype 2-D QMF satisfies the perfect or quasi-perfect reconstruction condition.

Since this method decomposes the design of an FCCS-type QMF into two problems, i.e., (i) design of the 2-D prototype QMF and (ii) determination of the value of k in (5), we can easily design FCCS-type QMFs for various subband shapes by suitably choosing coefficients of the prototype QMF and the value of k. Furthermore, the obtained analysis/synthesis filters can be implemented efficiently by using the 2-D Chebyshev structure [8].

3. Design of BCCS-Type QMF Banks

3.1 BCCS-type Downsampling

As one of the downsampling matrices for BCCS,

$$\boldsymbol{D}_{BCCS} = \begin{bmatrix} 1 & 1 & -1 \\ 1 & -1 & 1 \\ -1 & 1 & 1 \end{bmatrix} \quad (10)$$

can be used [8]. Since $L = |\det \boldsymbol{D}_{BCCS}| = 4$, the maximally-decimated QMF in this case has 4 channels.

To obtain a BCCS-type QMF bank, we utilize the fact that the downsampling matrix $\boldsymbol{D}_{BCCS}$ can be factored as

$$\begin{aligned} &\boldsymbol{D}_{BCCS} \\ &= \begin{bmatrix} 1 & 0 & 0 \\ 0 & 1 & -1 \\ -1 & 0 & 1 \end{bmatrix} \begin{bmatrix} 1 & 1 & 0 \\ 1 & 0 & 1 \\ 0 & 1 & 1 \end{bmatrix} \begin{bmatrix} 1 & 0 & 0 \\ 0 & 1 & -1 \\ 0 & 1 & 1 \end{bmatrix} \\ &\equiv \boldsymbol{E} \cdot \boldsymbol{D}_{FCCS} \cdot \begin{bmatrix} 1 & 0 & 0 \\ 0 & \multicolumn{2}{c}{\boldsymbol{D}_2} \\ 0 & & \end{bmatrix}. \end{aligned} \quad (11)$$

Since $|\det E| = 1$ in this case [7], the downsampling from the simple cubic sampling (SCS) to BCCS can be shown as in Fig. 4, where Fig. 4 (b) is obtained by the quincuncial downsampling with $\boldsymbol{D}_2$ followed by the FCCS-type downsampling with $\boldsymbol{D}_{FCCS}$. Indeed, a rotation of Fig. 4 (c) with respect to the axis n_1 by $-45°$ results in SCS with sampling period $1 : \sqrt{2} : \sqrt{2}$. If this SCS is then downsampled according to $\boldsymbol{D}_{FCCS}$, it would correspond to a transition from SCS to FCCS.

Figure 5 gives several possible baseband shapes for BCCS [10] (ω_{1c} has the same meaning as for the case of FCCS). By comparing Fig. 5 with Fig. 2, we can observe that Fig. 5 can be derived from Fig. 2 by using the transformation

$$\begin{bmatrix} \omega_1 \\ \omega_2 \\ \omega_2 \end{bmatrix} \leftarrow \begin{bmatrix} 1 & 0 & 0 \\ 0 & 1/2 & 1/2 \\ 0 & -1/2 & 1/2 \end{bmatrix} \begin{bmatrix} \omega_1 \\ \omega_2 \\ \omega_2 \end{bmatrix}. \quad (12)$$

Since the quincuncial downsampling involves $1/\sqrt{2}$ reduction and $-45°$ rotation in the ω_2–ω_2 plane, (12) corresponds to the relation between BCCS and FCCS shown in Fig. 4.

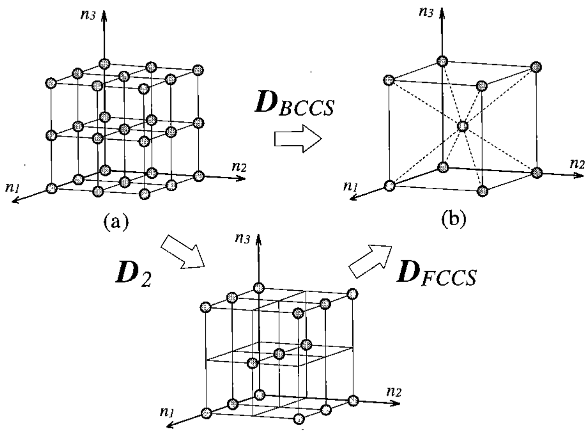

Fig. 4 BCCS-type downsampling.

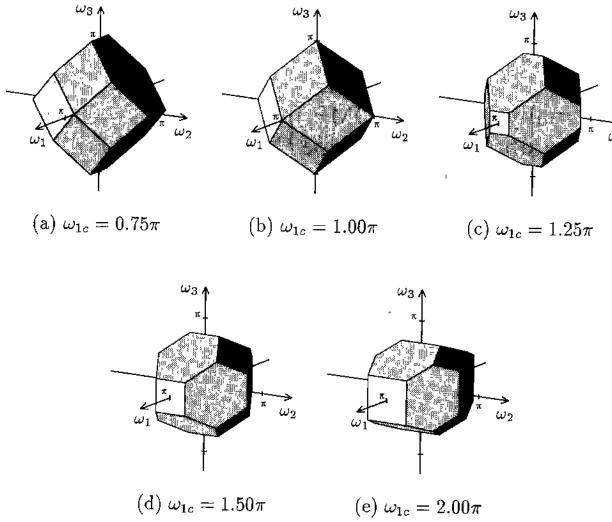

Fig. 5 Several possible baseband shapes for BCCS.

3.2 Proposed Design Method

In Refs. [8] and [10], the following design method for BCCS-type band-limiting filters has been proposed:

1. Design a suitable 2-D prototype filter $H(\omega_1, \omega)$ and a 2-D diamond-shaped filter $H'(\omega_2, \omega_2)$.
2. Obtain 3-D subfilter $H''(\omega_1, \omega_2, \omega_2) = H(\omega_1, \omega)\,|_{\cos\omega = F(\omega_2, \omega_2)}$ by applying the McClellan transformation with $k = 0.5$.
3. Rotate $H''(\omega_1, \omega_2, \omega_2)$ with respect to the axis ω_1 by -45° to obtain $H'(\omega_1, \omega_2, \omega_2)$.
4. Using the 2-D diamond-shaped filter $H'(\omega_2, \omega_2)$, suppress the unnecessary passbands, which appears as a result of the rotation in step 3.

The resulting band-limiting filter $H(\omega_1, \omega_2, \omega_2)$ is written as

$$H(\omega_1, \omega_2, \omega_2) = H'(\omega_2, \omega_2) \cdot H'(\omega_1, \omega_2, \omega_2)$$
$$= H'(\omega_2, \omega_2) \cdot H(\omega_1, \omega)|_{\cos\omega = F(\omega_2 - \omega_2, \omega_2 + \omega_2)} \quad (13)$$

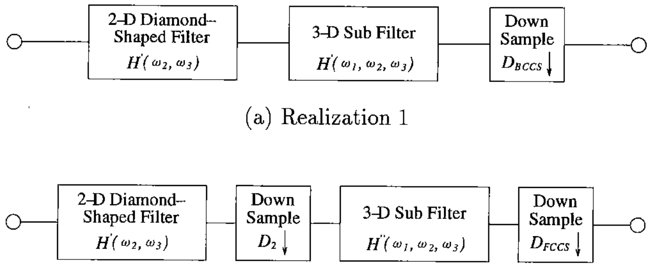

(a) Realization 1

(b) Realization 2

Fig. 6 Realization of BCCS-type band-limiting filters.

which is depicted as Fig. 6 (a). By using (11), Fig. 6 (a) can be equivalently transformed into Fig. 6 (b).

Now, the BCCS-type QMF bank can be easily designed by replacing the 2-D diamond-shaped filter and the FCCS-type band-limiting filter in Fig. 6 (b) with a suitable 2-D diamond-shaped two-channel QMF and an FCCS-type QMF, respectively. Figure 7 shows the resulting structure of the BCCS-type QMF banks, where $H_i(\omega_2, \omega_2)$ and $F_i(\omega_2, \omega_2)$ are the 2-D diamond-shaped analysis/synthesis filters, $H_i(\omega_1, \omega_2, \omega_2)$, $F_i(\omega_1, \omega_2, \omega_2)$ are the 3-D FCCS-type analysis/synthesis filters, $\boldsymbol{E}_{FCCS} = \boldsymbol{D}_{FCCS}$ and $\boldsymbol{E}_2 = \boldsymbol{D}_2$.

4. Design Examples

4.1 Design Example of FCCS-Type QMFs

In this example, the FCCS-type QMF of Fig. 2 (b) is designed. The ideal shape of each subband is shown in Fig. 8. This requires 2-D diamond-shaped QMF bank as its prototype [10]. In this paper, such a QMF bank is designed by using the method proposed in Ref. [13] with the following specifications;

Number of taps	:	7×7
Stopband	:	$\|\omega_1\| + \|\omega\| \geqq 1.68\pi$
Stopband attenuation	:	40 dB

An application of (7)–(8) to this 2-D prototype QMF completes the design procedure. -3 dB equi-amplitude surface of the designed subbnad L is shown in Fig. 9, where only the region $0 < \omega_2 < \pi$ is displayed.

4.2 Design Example of BCCS-Type QMFs

This section designs the BCCS-type QMF whose subband LL corresponds to Fig. 5 (b) (the first Brillouin zone). Since (12) converts Fig. 5 (b) into Fig. 2 (b), the FCCS-type QMF with the subband shape of Fig. 2 (b) is required, which has been designed in the previous example. For the required 2-D diamond-shaped two-channel QMF, the prototype for this FCCS-type QMF can be utilized.

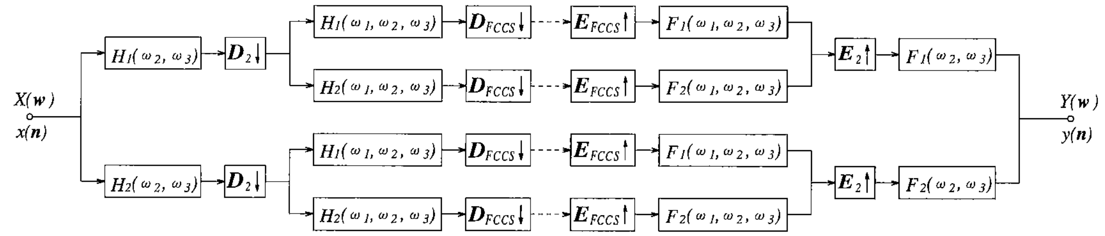

Fig. 7 Proposed structure for BCCS-type QMFs.

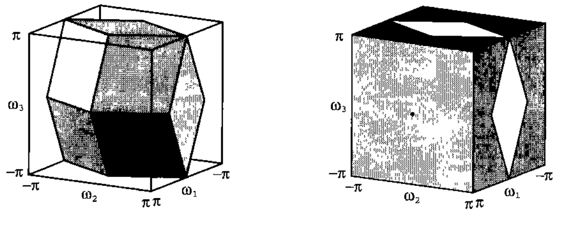

(a) Subband L (b) Subband H

Fig. 8 Ideal subband shapes of the FCCS-type QMF.

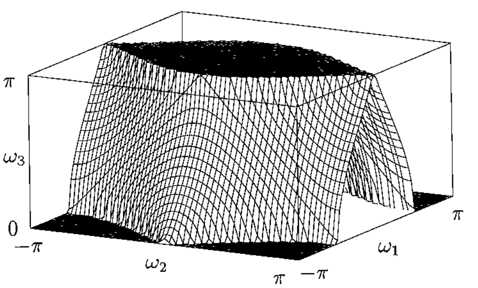

Fig. 9 −3 dB equi-amplitude surface of the subband L.

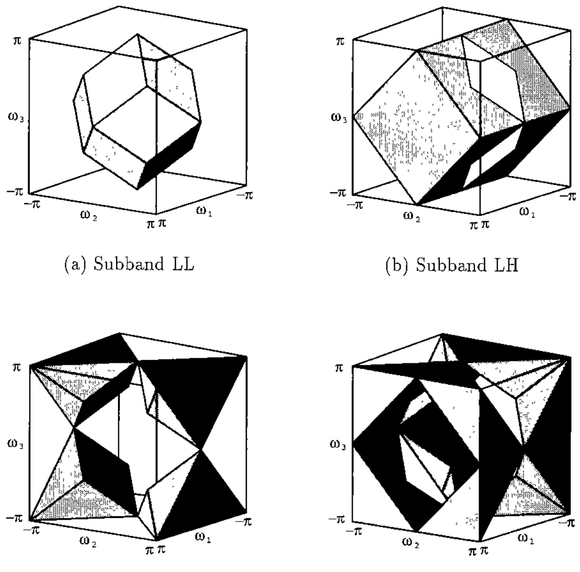

(a) Subband LL (b) Subband LH

(c) Subband HL (d) Subband HH

Fig. 10 Ideal subband shapes of the BCCS-type QMF.

Figures 10 and 11 show, respectively, the ideal shape of the four subbands, and −3 dB equi-amplitude surface of the designed subband LL. It can be observed from Fig. 11 that the designed subband has well approximated the ideal characteristics.

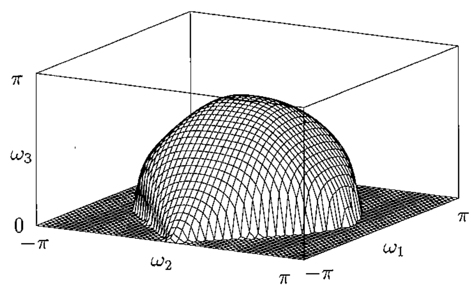

Fig. 11 −3 dB equi-amplitude surface of the subband LL.

5. Conclusions

In this paper, a design technique for 3-D FCCS and BCCS-types QMFs is proposed. Since the proposed technique decomposes the problem into designs of the 2-D prototype QMF and the 2-D McClellan transformation, the 3-D QMF bank can be easily designed. By using this technique, it is possible to realize various subband shapes as shown, for example, in Figs. 2 and 5. Furthermore, the designed filter banks can be implemented efficiently by using the 2-D Chebyshev structure.

A problem for further research is to investigate the subband shapes suitable for processing of image sequences.

References

[1] P.P. Vaidyanathan, "Multirate Systems and Filter Banks," Prentice-Hall, New Jersey, 1993.

[2] E. Chang and A. Zakhor, "Subband video coding based on velocity filters," Proc. 1992 IEEE ISCAS, pp.2288–2291, 1993.

[3] G. Karlsson and M. Vetterli, "Three dimensional subband coding of video," Proc. 1988 IEEE ICASSP, pp.1100–1103, 1988.

[4] J. Kovačević and M. Vetterli, "FCO sampling of digital video using perfect reconstruction filter banks," IEEE Trans. Image Proc., vol.2, no.1, pp.118–122, Jan. 1993.

[5] T. Chan and P.P. Vaidyanathan, "Multidimensional multirate filters and filter banks derived from one dimensional filters," IEEE Trans. Signal Proc., vol.41, no.5, pp.1749–1765, May 1993.

[6] G.J. Tonge, "Three-dimensional filters for television sampling," Experimental & Development Rep. 117/82, Independent Broadcasting Authority, June 1982.
[7] E. Dubois, "The sampling and reconstruction of time-varying imagery with application in video systems," Proc. IEEE, vol.73, no.4, pp.502–522, April 1985.
[8] T. Yoshida, A. Nishihara, and N. Fujii, "A design method for 3-Dimensional band-limiting FIR filters using McClellan transformation," IEICE Trans. Fundamentals, vol.E76-A, no.8, pp.1283–1292, Aug. 1993.
[9] T. Yoshida, A. Nishihara, and N. Fujii, "A design method of multidimensional half-band FIR filters using 2-D McClellan transformation and its applications," IEICE Tech. Rep., CAS93-25, May 1993 (in Japanese).
[10] K. Kamata, T. Yoshida, A. Nishihara, and N. Fujii, "Design of 3-D band-limiting filters," Proc. 1993 IEICE Spring National Convention, pp.1–158, March 1993 (in Japanese).
[11] J.D. Johnston, "A fulter family designed for use in quadrature mirror filter banks," Proc. 1980 IEEE ISCAS, pp.291–294, 1980.
[12] M. Ikehara, A. Yamashita, and H. Kurota, "Design of two-channel perfect-reconstruction QMF filter banks," Trans. IEICE, vol.J75-A, no.8, pp.1333–1340, Aug. 1992 (in Japanese).
[13] T. Yoshida, A. Nishihara, and N. Fujii, "Considerations on 2-D QMF filter banks," IEICE Tech. Rep., CAS90-34, June 1990 (in Japanese).